

# Cosmic Rays and Extensive Air Showers

Todor Stanev<sup>1</sup>

<sup>1</sup>Bartol Research Institute, Department of Physics and Astronomy, University of Delaware, Newark, DE 19716, U.S.A.

We begin with a brief introduction of the cosmic ray energy spectrum and its main features. At energies higher than  $10^5$  GeV cosmic rays are detected by the showers they initiate in the atmosphere. We continue with a brief description of the energy spectrum and composition derived from air shower data.

## 1 Introduction

Cosmic rays are defined as charged nuclei of non-solar origin, i.e. particles accelerated in the Galaxy or, at higher energy, in extragalactic astrophysical objects. The energy spectrum of the cosmic rays is a smooth power law spectrum  $F(E) = \text{const} \times E^{-\alpha}$  with only two identifiable features. The first one is the cosmic ray *knee* at about  $3 \times 10^6$  GeV where the spectrum steepens from  $\alpha = 2.7$  to 3.1 and the other one is the *ankle*, at about  $3 \times 10^9$  GeV, where the spectrum becomes again flatter.

The common wisdom is that cosmic rays below the knee are accelerated at galactic supernova remnants. Gamma-rays of energy up to 10 TeV have been observed from sources in the vicinity of well known supernova remnants which is an indication that these are indeed sources of cosmic rays acceleration. The acceleration spectra of cosmic rays are considerably flatter (with smaller  $\alpha$ ) than those of the cosmic rays at Earth. This is believed to be a propagation effect in the Galaxy, where the lower energy cosmic rays are contained for longer time. At energies above the cosmic ray knee we have no idea about the cosmic ray sources, except that the highest energy particles are certainly of extragalactic origin. It is remarkable that some astrophysical objects can accelerate particles to three orders of magnitude higher than the LHC equivalent

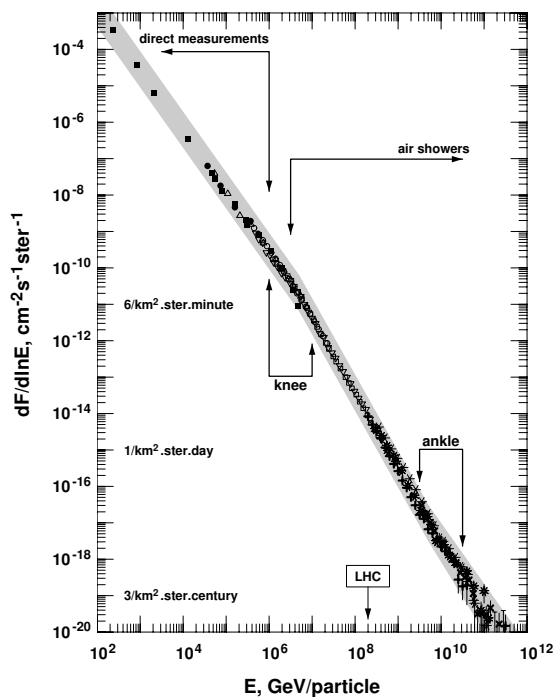


Figure 1: Cosmic rays energy spectrum above 100 GeV.

Lab energy.

The cosmic ray spectrum is shown in Fig. 1. The figure indicates the energy range where the cosmic ray spectrum is measured directly by balloon and satellite experiments. When the energy starts to exceed significantly 1,000 GeV the cosmic ray flux is too small and the cosmic rays are measured by the showers they generate in the atmosphere.

There are different types of air shower detectors:

- Air shower arrays consist of particle detectors that are spaced at different distances from each other depending on the energy range of the detectors. If the design is for detection of  $10^6$  GeV air showers the distance between detectors is several tens of meters. In the Auger southern observatory, which aims at shower energy exceeding  $10^9$  GeV the distance between detectors is 1,500 m. The shower arrays trigger when several detectors fire in coincidence. The reconstruction of the primary energy depends heavily of the hadronic interaction model that is used by the detector Monte Carlo simulation.
- Air Cherenkov detectors detect the Cherenkov light emitted by the shower charged particles (mainly electrons and positrons) in the atmosphere. Most of the light comes when the shower is at maximum.
- Fluorescent detectors detect the fluorescent light from the Nitrogen atoms in the atmosphere that are excited by the ionisation of the shower charged particles. Unlike the Cherenkov light the fluorescent light is isotropic. High energy showers can be observed from as far as 40 km away. Fluorescent detectors integrate over the shower longitudinal development to estimate the primary particle energy after adding the *invisible* energy, contained in high energy particles and neutrinos.

Different observational methods are now combined as in the case of the southern Auger observatory and the new Telescope Array detector.

## 2 Rough Estimates of the Shower Parameters

As mentioned earlier, shower Monte Carlo calculations are used for calculations of the efficiency of the detectors and estimations of its effective area. The main features of the air shower development can be understood on the basis of the *toy model* of the shower development created by Heitler [1]. Heitler assumed that the shower consists of one type of particles. At each interaction length  $\lambda$  two new particles are created each one of them carrying 1/2 of the energy. This continues until the particle energy is less than the critical energy  $E_c$  under which particles do not interact. The maximum number of particles in the cascade is then  $N_{max} = E_0/E_c$ . The depth of maximum is proportional to the logarithm of the ratio of the primary and the critical energies  $E_0/E_c$ :  $X_{max} = \lambda \log_2(E_0/E_c)$ .

Hadronic cascades are much more complicated but one can still use Heitler's approach to derive approximate expressions for some shower parameters. Assuming that the air shower development depends only on the first cosmic ray interaction, one can estimate the depth of the shower maximum in the atmosphere as [2]

$$X_{max} = X_0 \ln \left[ \frac{2(1 - K_{el})E_0}{((m)/3)\varepsilon_0} \right] + \lambda_N(E_0), \quad (1)$$

and the number of electrons at  $X_{max}$  as

$$N_e^{max} = \frac{1}{2} \frac{\langle m \rangle (1 - K_{el}) E_0}{3 \epsilon_0}, \quad (2)$$

where  $m$  is the effective meson multiplicity and the  $1/3$  factor accounts for the multiplicity of neutral mesons.  $K_{el}$  is the elasticity coefficient of the first interaction (roughly  $1/2$ ) and  $\epsilon_0$  is the critical energy of the electrons in air (81 MeV). Replacing the primary energy  $E_0$  with  $E_0/A$  (the mass of a nucleus) one can derive the expressions for showers initiated by primary nuclei. The conclusions are that  $X_{max}$  in such showers is smaller (showers develop higher in the atmosphere):  $X_{max}^A = X_{max}^p - X_0 \ln A$  and the muon/electron ratio in showers initiated by nuclei is higher by  $A^{1-\beta}$  ( $\beta = 0.85$ ) than in proton showers. These two parameters are most often used in studies of the cosmic ray chemical composition.

After this short introduction it is important to remember that cosmic ray shower experiments are observations, rather than experiments in the accelerator experiment sense. We have no idea of the energy and type of the primary particle or of the first interaction point in the atmosphere. We have to measure as many shower parameters as possible, compare them to Monte Carlo calculations, and derive the energy and composition of the primary particles. This not easy because of the large inherent fluctuations in the shower development. Figure 2 shows the shower longitudinal profiles of ten simulated proton showers of primary energy  $10^5$  GeV and their average.

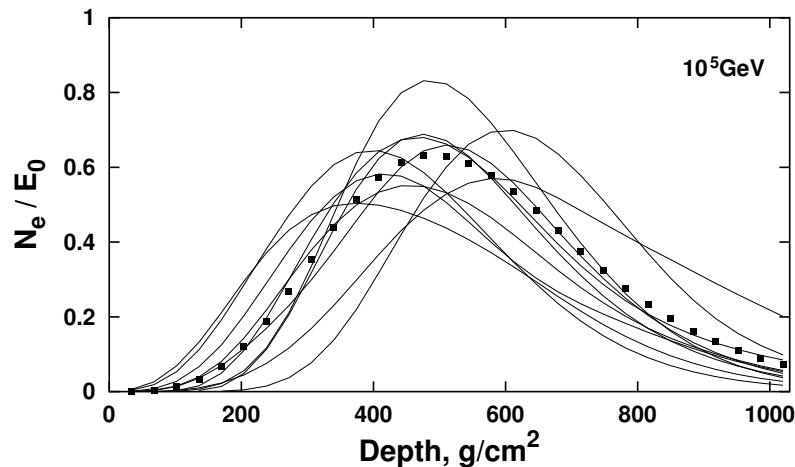


Figure 2: Shower profiles of ten simulated proton showers. The average shower profiles is shown with the points.

For this reason the reconstruction of individual showers is quite uncertain and we have to work with large statistical samples in the investigation of the cosmic ray energy spectrum and composition.

### 3 Air Shower Reconstruction and Analysis

The reconstruction of the air shower parameters starts with the determination of the position of the air shower core and the arrival direction of the air showers. Both these parameters require the knowledge of the lateral distribution of the air shower particles and the curvature of the air shower front.

The lateral distribution is strongly influenced by the type of the air shower detectors. Thin scintillator counters, for example, practically do not detect the gamma-rays in the air shower and count the shower electrons and muons the same way. Thick detectors, like the water Cherenkov tanks of Auger [3] and the frozen tanks of IceTop [4] convert the majority of the gamma-rays in electron-positron pairs. Muons generate much higher signals in such detectors.

Although the shower moves through the atmosphere with the speed of light its shape is not a plane. Particles deflected at large angles during the shower development have higher path lengths and arrive at the observation level slightly later and with more fluctuations. For these reasons the shower front is relatively thin in time close to the shower core (several nanoseconds) and considerably thicker at large distances from the core.

When all these effects are accounted for in an air shower array one uses them in an iterative procedure to calculate the exact position of the shower core from the lateral distribution of the shower particles and its arrival direction from the timing in the different detectors. The error in the shower core position is several meters and the direction has an error of about  $1^\circ$ .

The next step is the determination of the shower energy and primary particle mass. The shower energy is strongly correlated with the shower particles density (or signal strength) at certain distance from the core. The distance used is estimated for each detector as the position where the signal strength of showers from different nuclei fluctuates the least. It strongly depends on the distance between detectors and is usually slightly smaller than this distance.

The composition analysis is more complicated since it needs either the detection of the shower muons with underground (or well shielded) detectors or observation of the shower maximum with optical detectors. The showers with the smallest  $e/\mu$  ratio (or deeper  $X_{max}$  are from primary photons and the showers on the opposite side of the average are from heavy nuclei. The actual analysis procedure is different for each group but these basic principles are always used.

### 4 Experimental Data on the Cosmic Ray Energy Spectrum

Figure 1, which contains seventeen orders of magnitude in flux, gives the reader the impression that all measurements of the cosmic ray energy spectrum agree with each other. The truth is different, the air shower measurements (as well as the direct ones) do not agree very well with each other. Figure 3 demonstrates the current situation.

The cosmic rays spectrum shown in Fig. 3 is multiplied by  $E^{2.7}$  to emphasise the features in the energy spectrum, which are otherwise almost invisible. Such a presentation, however, significantly amplifies the differences between different experiments. A difference of 25% (typical systematic uncertainty) in the energy estimate of two experiments leads to a visible difference of 1.5 in the presented spectrum plus a shift in the energy scale. The biggest differences in Fig. 3 are in two energy ranges: just before the cosmic ray knee, and at energies higher than  $10^9$  GeV. In the lower energy range most of the errors should be systematic as for many experiments this

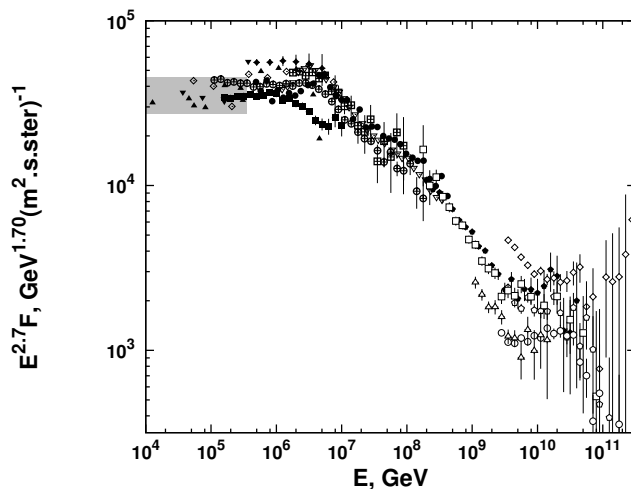


Figure 3: Cosmic ray energy spectrum measured by different air shower experiments [6]. The only set of direct measurements is shown with filled squares.

is either the beginning or the end of their sensitivity range. For these reasons the exact position of the cosmic ray knee is not determined.

A highly respected analysis of the cosmic ray knee region comes from the Kascade group [5]. The shower array Kascade consists of 252 electron and muon detectors covering an area of  $200 \times 200 \text{ m}^2$  with a  $320 \text{ m}^2$  calorimeter in the middle. The primary energy estimate is a combination of weighted electron and muon numbers in the shower. The basis of the analysis is a two dimensional  $N_e$  and  $N_\mu$  distribution of all detected showers above the threshold  $N_e$  and  $N_\mu$  values. Since showers generated by different primary nuclei this distribution was used to generate the energy spectra of the different components, and thus the energy dependence of the cosmic ray chemical composition. The collaboration paid much attention to the results using two different hadronic interaction models for the analysis.

If the interaction model QGSjet01 [7] were used the knee of the all nuclei cosmic ray spectrum is at  $4 \times 10^6 \text{ GeV}$  and the two spectral indices before and after the knee are 2.7 and 3.1. In the case of SIBYLL 2.1 [8] the knee is at  $5.7 \times 10^6 \text{ GeV}$  and the spectral indices are the same. The energy spectra of the individual five components (H, He, C, Si, Fe) show a domination of the heavy nuclei at energy above  $2 \times 10^7 \text{ GeV}$  while before the knee the spectra of He and H have the highest fluxes. It was not possible to derive exactly the *knees* of the individual components. The calculations with the Sibyll interaction model show a slightly heavier nuclear composition.

At much higher energy (above  $10^{10} \text{ GeV}$ ) there are very different measurements of the cosmic ray flux. The highest values were obtained by the AGASA experiment [9], which published eleven events with energy exceeding  $10^{11} \text{ GeV}$ . More recently these events were re-analyzed with the standard hadronic interaction models and the energy estimate was decreased. The highest statistics measurements are those of the High Resolution Fly's Eye (HiRes) and especially the Auger Southern Observatory.

Both HiRes and Auger observed the GZK [10] cutoff of the cosmic ray spectrum [11, 12] that is caused by the interactions of the ultrahigh energy cosmic rays (UHECR) with the mi-

crowave background (MBR). The UHECR energy is so high that photoproduction interactions are possible in the MBR for cosmic rays of energy above  $3 \times 10^{10}$  GeV. The energy loss length of  $10^{11}$  GeV protons is of order 100 Mpc ( $3 \times 10^{24}$  m) and decreases to about 15 Mpc at higher energy. Heavy nuclei lose energy in photodisintegration, where they lose one or two nucleons per interaction. Since the required CMS energy is much smaller the interaction starts at much smaller energy per nucleon,  $E^0/A$ . UHE gamma-rays lose energy even faster than protons. These distances define the GZK horizon within which we look for the sources of UHECR.

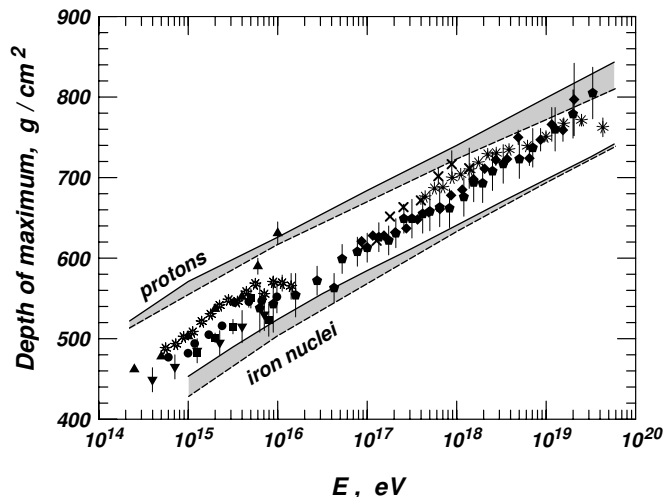


Figure 4: Depth of maximum measurements as a function of the shower energy. The shaded areas are the predictions of different models for protons and iron nuclei.

The chemical composition of UHECR is not well established yet. At these energies the composition is measured by the depth of shower maximum ( $X_{max}$ ). HiRes measures  $X_{max}$  consistent with pure proton composition of UHECR, while Auger sees  $X_{max}$  distributions indicating medium heavy nuclei such as Oxygen or Carbon as shown in Fig. 4. Our previous expectations were that extragalactic cosmic rays would mostly consist of protons with a 10% admixture of He nuclei in accordance with the average composition of extragalactic matter.

If the cosmic ray composition measured by Auger is confirmed we will have to look for the sources of the ultrahigh energy cosmic rays among the astrophysical objects where there are enough heavy nuclei to become accelerated. On the other hand heavy nuclei have a maximum acceleration energy higher by the charge  $Z$  from that of protons.

## Acknowledgements

This short review comes from work performed in collaboration with P.L. Biermann, R. Engel, T.K. Gaisser, A. Reimer, D. Seckel and others. Partial support for my work comes from the US Department of Energy contract DE-FG02-91ER40690.

## References

- [1] W. Heitler, Quantum Theory of Radiation (Oxford University Press, 1944)
- [2] J. Matthews, Astropart. Phys., **22**, 387 (2005)
- [3] See <http://auger.org>
- [4] X. Bai for the IceCube collaboration, Nucl. Phys. B (Proc. Suppl) **175**, 415 (2008)
- [5] T. Antoni et al, Astropart. Phys. 24:1 (2005)
- [6] T.K. Gaisser and T. Stanev, Cosmic Rays, in Review of Particle Physics. Particle Data Group (C. Amsler et al.), Phys.Lett.B**667**:1 (2008)
- [7] N.N. Kalmykov, S.S. Ostapchenko & A.I. Pavlov, Nucl. Phys. B (Proc. Suppl.), **52B**, 17 (1997)
- [8] R. Engel et al., Proc. 26th Int. Cosmic Ray Conf. (Salt Lake City), **1**, 415 (1999)
- [9] M. Takeda et al., Phys. Rev. Lett., **81**, 1163
- [10] K. Greisen, Phys. Rev. Lett., **16**, 748 (1966); G.T. Zatsepin & V.A. Kuzmin, JETP Lett. **4** 78 (1966)
- [11] R. Abbasi et al. (HiRes Collaboration), Phys. Rev. Lett. **100**:101101 (2008)
- [12] J. Abraham et al. (Auger Collaboration), Phys. Rev. Lett. **101**:061101 (2008)